Object Recognition Using Radon Transform-Based RST Parameter Estimation

Nafaa Nacereddine[1], Salvatore Tabbone[2], and Djemel Ziou[3]

[1] DTSI, Centre de Recherche en Soudage et Controle, 16002 Algiers, Algeria
nafaa.nacereddine@enp.edu.dz
[2] Université Nancy 2-Loria, BP 239, 54506 Vandoeuvre-lès-Nancy, France
tabbone@loria.fr
[3] Dépt. d'informatique, Univ. de Sherbrooke, Qc., Canada J1K 2R1
djemel.ziou@usherbrooke.ca

Abstract. In this paper, we propose a practical parameter recovering approach, for similarity geometric transformations using only the Radon transform and its extended version on $[0, 2\pi]$. The derived objective function is exploited as a similarity measure to perform an object recognition system. Comparison results with common and powerful shape descriptors testify the effectiveness of the proposed method in recognizing binary images, RST transformed, distorted, occluded or noised.

Keywords: RST parameters, Radon transform, object recognition.

1 Introduction

The shape is an important visual feature for object description, unavoidable in object recognition and image retrieval tasks. Object description techniques are extensively studied in literature (e.g. [1]) and broadly divided in two groups: contour-based and region-based shape descriptors. Within this last category, an increasing and recent interest is devoted to shape descriptors using the Radon transform (e.g. [2],[3],[4],[5]), because of its richness in information. The Radon transform (RadTr), since its introduction in the beginning of the last century, has long been studied and applied by researchers in great number of applications, especially in the biomedical imaging field, where the obtained raw data are often sinograms. By using the Radon transform properties regarding usual geometric transformations of rotation, scaling and translation (RST), it is question to recover the parameters of such transformations, by handling only the image projections assuming no access to the spatial domain of image. In [6], the authors present a method for the transformation parameter recovering of a binary object subjected to reflection, scaling, translation and rotation using only the Radon projections. Nevertheless, the objective function used for the computation of the rotation angle is not valid for any angle of rotation belonging to the range $[0, 2\pi]$, as it will be shown in Sect. 3. In [7], the authors use the results obtained in [6] but develop a novel method for parameter decoupling and an improved phase correlation method for accurate shift estimation, resulting in a

J. Blanc-Talon et al. (Eds.): ACIVS 2012, LNCS 7517, pp. 515–526, 2012.

fast matching algorithm. However, the rotation angle estimation is slightly less accurate compared to [6]. In this paper, in Sect. 4., we develop a step-by-step method with the aim to estimate the RST transform parameters brought into play between to unknown images, where we construct a 2π-based Radon transform to deal with the problem of rotation by any angle comprising in $[0, 2\pi]$. Results of this part are given in Sect. 5.1. Moreover, at Sect. 5.2., an object recognition system is proposed, using the Radon-based paradigm developed in the previous section.

2 Object Subjected to RST Transformations

Assume f an image in $x-y$ plane, subjected to a sequence of geometric transformations of rotation R_{ϕ_0}, scaling S_α and translation T_{x_0,y_0}, where ϕ_0 (in $[0, 2\pi]$), α (in $\mathbb{R}_+$) and (x_0, y_0) (in $\mathbb{R}^2$) are, respectively, the rotation angle, the scaling factor and the translation vector components. The result is a transformed image, noted g with coordinates x', y', as shown in Fig. 1. This composition of transformations can be formulated as

$$\begin{cases} x' = \alpha(\cos\phi_0 x - \sin\phi_0 y) + x_0 \\ y' = \alpha(\sin\phi_0 x + \cos\phi_0 y) + y_0 \end{cases} \tag{1}$$

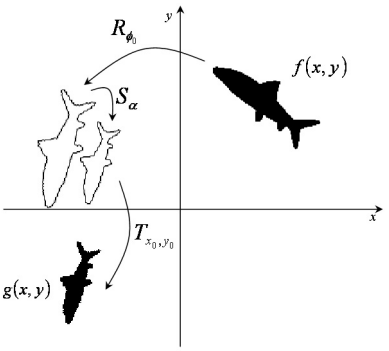

Fig. 1. A binary image rotated, scaled and translated

3 Radon Transform and Its Properties

Let L be a straight line in the $x-y$ plane and ds be an increment of length along L, the Radon transform [8] of a real valued function f, denoted $f^\vee$, is defined by its integral as

$$f^\vee(p, \phi) = \int_L f(x, y)ds \tag{2}$$

$f^{\vee}(p,\phi)$ is then determined by integration of all lines $L_{p,\phi}$, in the $x-y$ plane, $p \in \mathbb{R}, \phi \in [0,\pi]$. From Fig. 2, the equation of L is written as $p = x\cos\phi + y\sin\phi$. If we rotate the coordinate system by an angle ϕ, and label the new axes p and s, we obtain $x = p\cos\phi - s\sin\phi$, $y = p\sin\phi + s\cos\phi$. Then, $f^{\vee}$ is defined by

$$f^{\vee}(p,\phi) = \int_{-\infty}^{\infty} f(p\cos\phi - s\sin\phi, p\sin\phi + s\cos\phi)ds \tag{3}$$

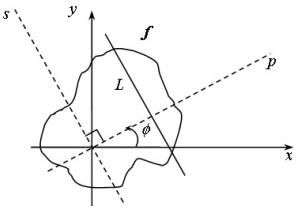

Fig. 2. Definition of the Radon transform

The Radon transform has several useful properties [8]. We give here those that are relevant for our application :

- *Periodicity*: $f^{\vee}(p,\phi) = f^{\vee}(p,\phi \pm 2k\pi)$, $k \in \mathbb{Z}$
- *Symmetry*: $f^{\vee}(p,\phi) = f^{\vee}(-p,\phi \pm (2k+1)\pi)$, $k \in \mathbb{Z}$
- *Translation by a vector* $\boldsymbol{u} = (x_0, y_0)$: Let $g = T_{\boldsymbol{u}}(f)$ then $g^{\vee}(p,\phi) = f^{\vee}(p - x_0\cos\phi - y_0\sin\phi, \phi)$
- *Rotation by an angle* ϕ_0: Let $g = R_{\phi_0}(f)$ then $g^{\vee}(p,\phi) = f^{\vee}(p,\phi - \phi_0)$
- *Scaling by a factor* α $(\alpha > 0)$: Let $g = S_{\alpha}(f)$ then $g^{\vee}(p,\phi) = \alpha f^{\vee}(p/\alpha,\phi)$

Before going any further, let us examine in details the rotation properties where modifications will be brought to make the algorithm proposed in the next section efficient in the object recognition task.

Let be f_r the function representing the rotated object by an angle ϕ_0 ($\phi_0 \in [-\pi,\pi]$), i.e. for any (x,y) belonging to $\mathbb{R}^2$,

$$f_r(x,y) = f(\cos\phi_0 x - \sin\phi_0 y, \sin\phi_0 x + \cos\phi_0 y) \tag{4}$$

In the rest of this section, we assume that the object is centered, i.e. the object is translated so that its centroid coincides with the $x-y$ plan origin O. This assumption is taken to avoid the translation effect introduced by the rotation, since only the rotation property, properly named, will be examined. It can be shown that the rotation property of the Radon transform displayed on $[0,\pi]$ obeys to the following equations
for $\phi_0 \in [-\pi, 0]$

$$f_r^{\vee}(p,\phi) = \begin{cases} f^{\vee}(-p,\phi - \phi_0 - \pi) & \text{if} \quad \phi \geq \phi_0 + \pi \\ f^{\vee}(p,\phi - \phi_0) & \text{if} \quad \phi \leq \phi_0 + \pi \end{cases} \tag{5}$$

for $\phi_0 \in [0, \pi]$

$$f_r^{\vee}(p,\phi) = \begin{cases} f^{\vee}(-p, \phi - \phi_0 + \pi) & \text{if} \quad \phi \leq \phi_0 \\ f^{\vee}(p, \phi - \phi_0) & \text{if} \quad \phi \geq \phi_0 \end{cases} \tag{6}$$

In Fig. 3, an example explaining the above equations is given. Then, as it can be seen, the rotation property of the Radon transform often given in the literature ($f_r^{\vee}(p,\phi) = f^{\vee}(p, \phi - \phi_0)$) is only valid if $\phi_0 \leq \phi \leq \phi_0 + \pi$.

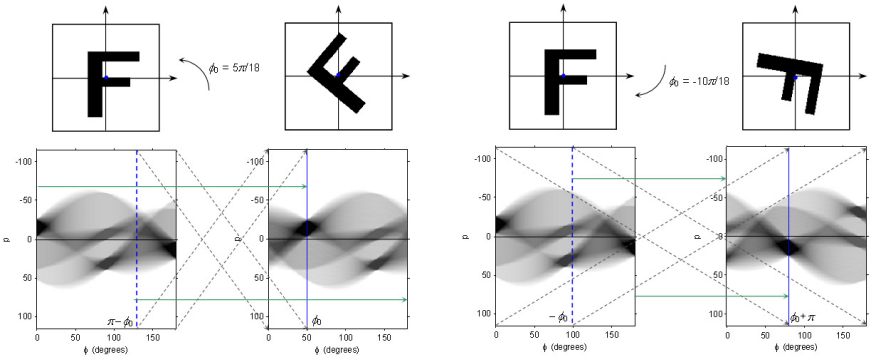

Fig. 3. Rotation property of Radon transform defined on π: if $\phi_0 \in [-\pi, 0]$ then $f_r^{\vee}(p, 0 : \phi_0 + \pi) = f^{\vee}(p, -\phi_0 : \pi)$ and $f_r^{\vee}(p, \phi_0 + \pi : \pi) = f^{\vee}(-p, 0 : -\phi_0)$; however, if $\phi_0 \in [0, \pi]$ then $f_r^{\vee}(p, 0 : \phi_0) = f^{\vee}(-p, \pi - \phi_0 : \pi)$ and $f_r^{\vee}(p, \phi_0 : \pi) = f^{\vee}(p, 0 : \pi - \phi_0)$

Besides its circular shifting in the variable ϕ, the complete rotation property of Radon transform will be related to the symmetry property of this latter. For this reason, an extended version of Radon transform (see Fig. 4) is proposed in (7) which is derived from the above equations so that, the rotation property of the new version of Radon transform will be simply and globally defined of any object rotation angle belonging to $[0, 2\pi]$

$$f_{2\pi}^{\vee}(p,\phi) = \begin{cases} f^{\vee}(p, \phi) & \text{if} \quad \phi \in [0, \pi] \\ f^{\vee}(-p, \phi) & \text{if} \quad \phi \in]\pi, 2\pi] \end{cases} \tag{7}$$

and the 2π-based Radon transform of the rotated object is expressed as

$$f_{r2\pi}^{\vee}(p,\phi) = \begin{cases} f_{2\pi}^{\vee}(p, \phi - \phi_0) & \text{if} \quad \phi \geq \phi_0 \\ f_{2\pi}^{\vee}(p, \phi - \phi_0 + 2\pi) & \text{if} \quad \phi \leq \phi_0 \end{cases} \tag{8}$$

which can be written as $f_{r2\pi}^{\vee}(p,\phi) = f_{2\pi}^{\vee}(p, \phi - \phi_0)$, since Radon transform is 2π periodic. As shown in Fig. 4, the rotation is transformed in circular shifting on [0 2π]. Consequently, the 2π-based Radon transform will be employed in the next section in the computation of the objective function leading to the estimation of the rotation angle between two compared images via their sinograms. According to the Radon transform definition and the symmetry property, the part of transform below to zero can be omitted.

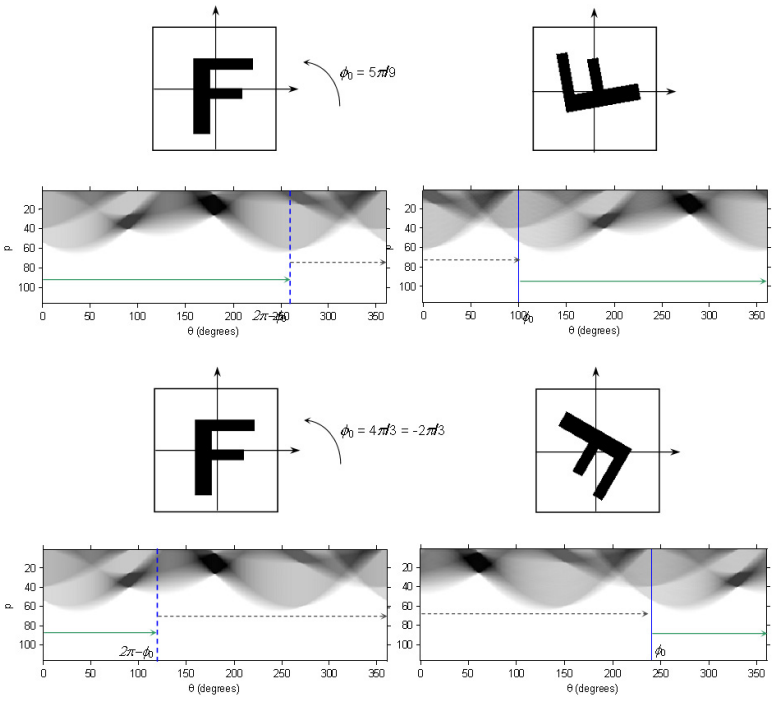

Fig. 4. Rotation property of RadTr represented on 2π: A rotation of the image by an angle ϕ_0 implies a shifting of the 2π-based Radon transform of ϕ_0 modulo 2π

4 Recover RST Parameters Using Radon Transform

To be useful, a shape recognition framework should allow explicit invariance under RST operations. To measure the similarity between the Radon matrix of two shapes, it is necessary to know the underlying geometric transformations from one shape into the other. We can see from the Radon transform properties that if a given shape is RST transformed, it will be difficult to recover all the RST parameters using only the quoted transform. To circumvent this situation, we propose a step-by-step RST parameter recovering, handling only the source and target object Radon projections.

(a) **Input data**: Source image f and target image g.

(b) **Output**: Transform parameters $\alpha, \boldsymbol{u}(x_0, y_0), \phi_0^*$ and similarity measure $F(\phi_0^*)$.

(c) Compute the RadTrs $f^\vee$ and $g^\vee$. Deduce the scaling parameter α as in [6]

$$\alpha = \left| \frac{\int_{-\infty}^{+\infty} g^\vee(p,\phi)dp}{\int_{-\infty}^{+\infty} f^\vee(p,\phi)dp} \right|^{1/2} \tag{9}$$

for any angle, ϕ.

(d) The coordinates of the centroids can be computed in terms of the Radon transforms $f^{\vee}$ and $g^{\vee}$. Indeed, by using (3) and the rotation Radon transform property for $\phi_0 = \pi/2$, (x_f, y_f) can be expressed, for any ϕ, by

$$\begin{cases} x_f = \frac{\int_{-\infty}^{+\infty} pf^{\vee}(p,\phi)dp}{\int_{-\infty}^{+\infty} f^{\vee}(p,\phi)dp}\cos\phi - \frac{\int_{-\infty}^{+\infty} pf^{\vee}(p,\phi+\pi/2)dp}{\int_{-\infty}^{+\infty} f^{\vee}(p,\phi)dp}\sin\phi \\ y_f = \frac{\int_{-\infty}^{+\infty} pf^{\vee}(p,\phi)dp}{\int_{-\infty}^{+\infty} f^{\vee}(p,\phi)dp}\sin\phi + \frac{\int_{-\infty}^{+\infty} pf^{\vee}(p,\phi+\pi/2)dp}{\int_{-\infty}^{+\infty} f^{\vee}(p,\phi)dp}\cos\phi \end{cases} \tag{10}$$

where x_f and y_f can be computed for several values of ϕ and the results are averaged. Analogously, the above formula is used to compute the mass center coordinates (x_g, y_g) for the function g.

(e) Compute the RadTrs of f and g, centered at the axes system origin, using the translation property of the RadTr. The components of the displacement vectors are then given by $\boldsymbol{u}_f(-x_f, -y_f)$ and $\boldsymbol{u}_g(-x_g, -y_g)$ for f and g, respectively. Then, the RadTr of the centered images f_c and g_c are given by:

$$\begin{cases} f_c^{\vee}(p,\phi) = f^{\vee}(p + x_f\cos\phi + y_f\sin\phi, \phi) \\ g_c^{\vee}(p,\phi) = g^{\vee}(p + x_g\cos\phi + y_g\sin\phi, \phi) \end{cases} \tag{11}$$

(f) Compute the RadTr on 2π for the centered images $f_{c2\pi}^{\vee}$ and $g_{c2\pi}^{\vee}$ using (7).

(g) Compute $f_{c2\pi}^{\vee}$ normalized in size to $g_{c2\pi}^{\vee}$

$$f_{c2\pi}^{\vee s}(p,\phi) = \alpha f_{c2\pi}^{\vee}\left(\frac{p}{\alpha}, \phi\right) \tag{12}$$

(h) Compute the optimal rotation angle ϕ_0^* (in $[0, 2\pi]$) given by the minimal value of the following objective function

$$F(\phi_0) = \int_0^{2\pi}\int_{-\infty}^{\infty} |g_{c2\pi}^{\vee}(p,\phi) - f_{c2\pi}^{\vee s}(p, \phi - \phi_0)|\, dp\, d\phi \tag{13}$$

and then, $\phi_0^* = \arg\min_{\phi_0} F$.

(i) Deduce from (1) the coordinates of the translation vector $\boldsymbol{u}(x_0, y_0)$

$$\begin{cases} x_0 = x_g - \alpha\cos\phi_0^* x_f + \alpha\sin\phi_0^* y_f \\ y_0 = y_g - \alpha\sin\phi_0^* x_f - \alpha\cos\phi_0^* y_f \end{cases} \tag{14}$$

5 Experiments

The first experiment will consist in the implementation of the proposed algorithm to recover the parameters of RST operation sequence applied on a real binary

image. The second experiment will be conducted using such algorithm, for an object recognition purpose.

5.1 RST Parameters Recovering

The implementation of the proposed algorithm on the 200×200 fish image of Fig. 1 can be summarized in Fig. 5 where real RST transform parameters are: $\phi_0 = 5\pi/9$, $\alpha = 0.7$, $\boldsymbol{u}(x_0, y_0) = (-10, -30)$, and the estimated ones are: $\hat{\phi}_0 = 5\pi/9$, $\hat{\alpha} = 0.701$, $\hat{\boldsymbol{u}}(x_0, y_0) = (-10.09, -29.98)$. In Table 1, we compare the proposed algorithm with that of [7] on recognizing the Shepp-Logan head phantom test image [9] (Fig. 6). The symbol s in [7] represents $1/\alpha$ in this paper.

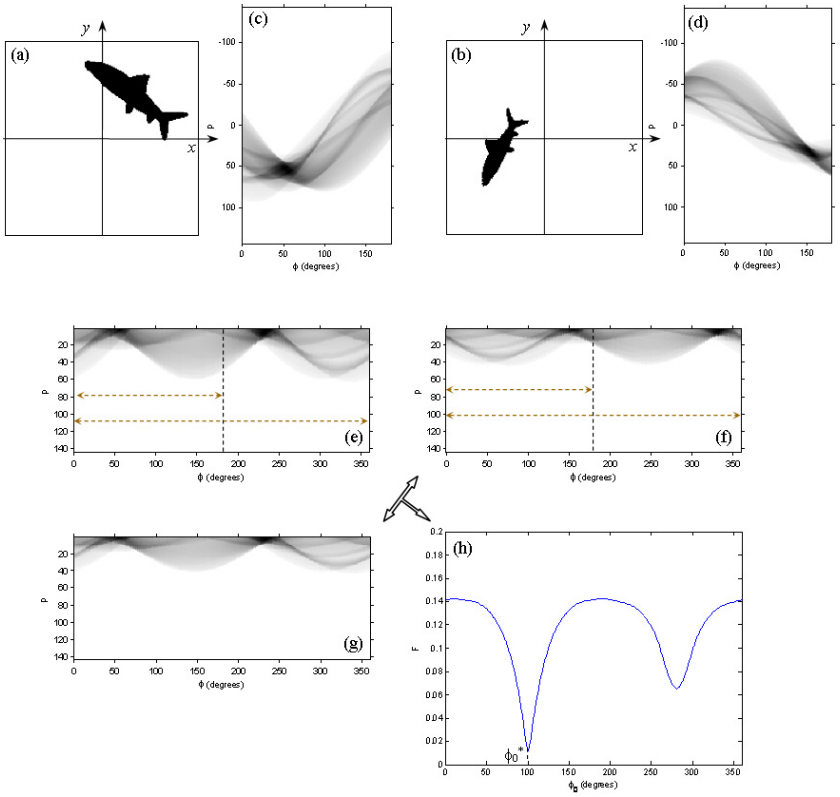

Fig. 5. RST parameter compuation using Radon transform. (a) Original fish image f. (b) The RST transformed image g with $\phi_0 = 5\pi/9$, $\alpha = 0.7$, $\boldsymbol{u}(-10, -30)$. (c) and (d) f and g RTs, resp. (e),(f) and (g) 2π-based RadTr of f centered, g centered and f centered and scaled, resp. (h) Objective function F where $\phi_0^* = 100° \sim 5\pi/9$.

Contrary to the proposed method, where the rotation angle estimate $\hat{\phi}_0$ (in $[0, 2\pi]$) can be obtained directly by (13), we note that for the work in [7], the

Fig. 6. Shepp-Logan head phantom test image of size 128×128

Table 1. Performance comparison between the algorithm in [7] and the proposed algorithm

Initial parameters				Algorithm in [7]				Proposed algorithm			
(x_0, y_0)	s	α	ϕ_0	$(\hat{x}_0, \hat{y}_0)$	$\hat{s}$	$\hat{\alpha}$	$\hat{\phi}_0$	$(\hat{x}_0, \hat{y}_0)$	$\hat{s}$	$\hat{\alpha}$	$\hat{\phi}_0$
(11 -5)	1	1	20	(10.32 -4.87)	1.00	1	20	(11.04 -4.99)	1.00	1	20
(-3 -12)	1.1	0.91	236	(-2.61 -11.50)	1.09	0.92	236	(-3.04 -12.04)	1.10	0.91	236
(-6 -2)	0.7	1.43	231	(-5.79 -1.76)	0.70	1.43	231	(-6.13 -2.12)	0.70	1.43	231
(-1 11)	1.2	0.83	260	(-0.75 11.67)	1.20	0.83	259	(-1.67 11.19)	1.20	0.83	260
(13 -12)	0.6	1.67	322	(12.82 -11.75)	0.60	1.67	322	(12.90 -11.74)	0.60	1.67	322
(-11 -15)	1.3	0.77	236	(-10.83 -13.89)	1.28	0.78	235	(-10.79 -15.36)	1.30	0.77	236
Mean error ($\times 10^{-3}$)				(3.13 4.88)	4.1	4.0	8.1	(1.15 1.63)	0.3	0.6	0

method for estimating ϕ_0 cannot distinguish between ϕ_0 and $\phi_0 + \pi$. According to the author, a way to get around this problem is to treat the two cases separately and choose the angle that produce a better match between the original an the estimated sinograms. The results given in Table 1 show that the proposed method is more accurate than the method in [7] for the estimation of the various RST parameters. In the other hand, for [6], the objective function used for the estimation of the rotation angle is not enough explicit to deal with any rotation angle value.

5.2 Object Recognition

The application of the proposed algorithm to object recognition is divided into two steps. The first step involves recovering the scaling parameter α and computing RadTrs of the centered images for any two shape images I and J, taken from the image database. The second step consists in measuring the similarity between I and J by computing the distance which gives the minimum value of F versus ϕ_0.

$$F(I, J, \phi_0) = \int_0^{2\pi} \int_0^{\infty} \left| J^{\vee}_{c2\pi}(p, \phi) - \alpha I^{\vee}_{c2\pi}\left(\frac{p}{\alpha}, \phi - \phi_0\right) \right| dp\, d\phi \tag{15}$$

and then,

$$dist(I, J) = \min_{\phi_0} F(I, J, \phi_0) \tag{16}$$

In order to demonstrate the effectiveness of the proposed descriptor, named RST-$\Re$, in object recognition, two experiments have been carried out on two binary image databases. Firstly, RST-$\Re$ is implemented and compared with other

descriptors on Shapes99 database [10] (Fig. 7), which is composed of 99 shapes, grouped in 9 categories with 11 shapes per category, and which is used to evaluate its robustness to occlusion, variations in form, missing parts and elastic deformation. Moreover, some samples are scaled and rotated. Secondly, the robustness to noise of the proposed descriptor is tested on the a set of datasets generated from the UMD Logo dataset [11] by adding noise of different levels to its images (Fig. 8). Each of these six logo datasets has 80 images of 10 categories, each of them contains 8 images generated by randomly scaling, rotating, translating the corresponding logo image. The "salt & peeper" noise density, noted d, consists in the percentage of the corrupted pixel in the image. This noise is added to each image with different densities ranging from 0 (noiseless image) to 0.20 with an increment of 0.04. For both shape image databases, RST-$\Re$ is compared to five region-based shape descriptors: Hu moments [12], Zernike moments [13], Generic Fourier Descriptor (GFD) [14], Radon Composite Features (RCF) [4] and Wavelet $\Phi\Re$-signature (W$\Phi\Re$) [5]. The criterion used for comparison among descriptors is the precision-recall curve used in the information retrieval context. In their simplest definition, precision (Pr) is the proportion of retrieved images that are relevant, and recall (Re) is the proportion of relevant images that are retrieved. To compute the precision-recall curve for each database, in the experiment, each of the images in the database is used as a query to which all the images in the database are compared with. The comparison is carried out using the similarity measure for RST-$\Re$ given by (16); whereas, for the other descriptors and for any two shape images I and J, the similarity measure is defined, as the ℓ_1-norm distance

$$dist(I, J) = \|D(I) - D(J)\|_1 \tag{17}$$

where D is the shape descriptor to which RST-$\Re$ is compared with.

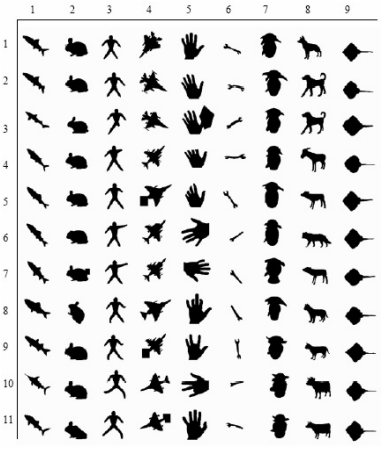

Fig. 7. Images of database "Shapes99"

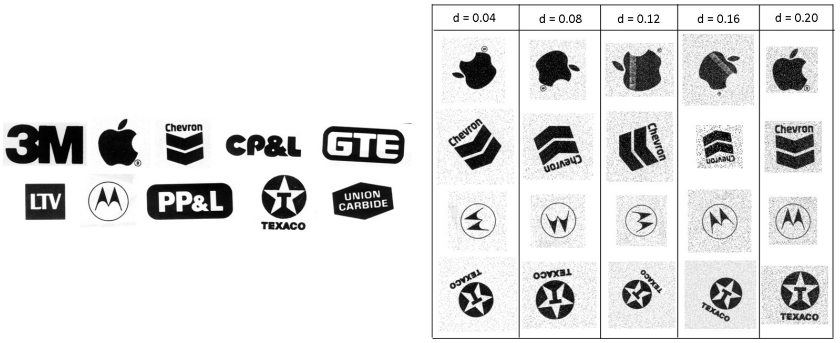

Fig. 8. (Left) Ten logo images from the UMD Logo database (noise-free images representing the first dataset). (Right) Sample of noisy images generated with d = 0.04, 0.08, 0.12, 0.16, 0.20 corresponding to the five noisy datasets.

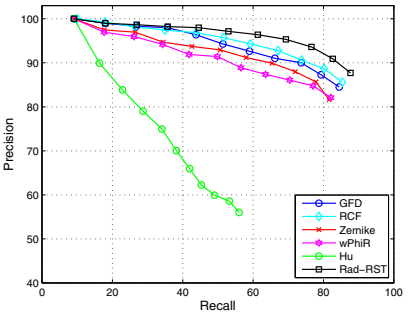

Fig. 9. $Pr - Re$ curves of comparison descriptors on the "Shapes99" database

According to the retrieval results provided in Fig. 9, it appears that $\Re$-RST outperforms all the other descriptors for shapes subjected to distortion, occlusion and deformation as in the case of Shapes99 database. Indeed, the Radon transform is not only lossless but rich in information, the reason for which $\Re$-RST exploiting the entire Radon projections is better than descriptors using spatial information such as GFD, Zernike or Hu descriptors. Moreover, the proposed descriptor is more powerful than RCF and W$\Phi\Re$ which may have loss of information due to the compression process from the 2D Radon image to 1D signatures. According to retrieval results given for logo datasets in Fig. 10, we note that all descriptors have ideal performance for the noiseless dataset, i.e. d=0 (top-left graph). However, the performance of other descriptors decreases proportionally to noise density (Fig. 10) while $\Re$-RST performs well due to robustness to additive noise of the Radon transform (Refer to [15] for detailed proof). Another important issue is computational complexity. The major part of computational time of $\Re$-RST is spent in the minimization of the similarity measure which may be high; however, it is largely dependent on how big the image

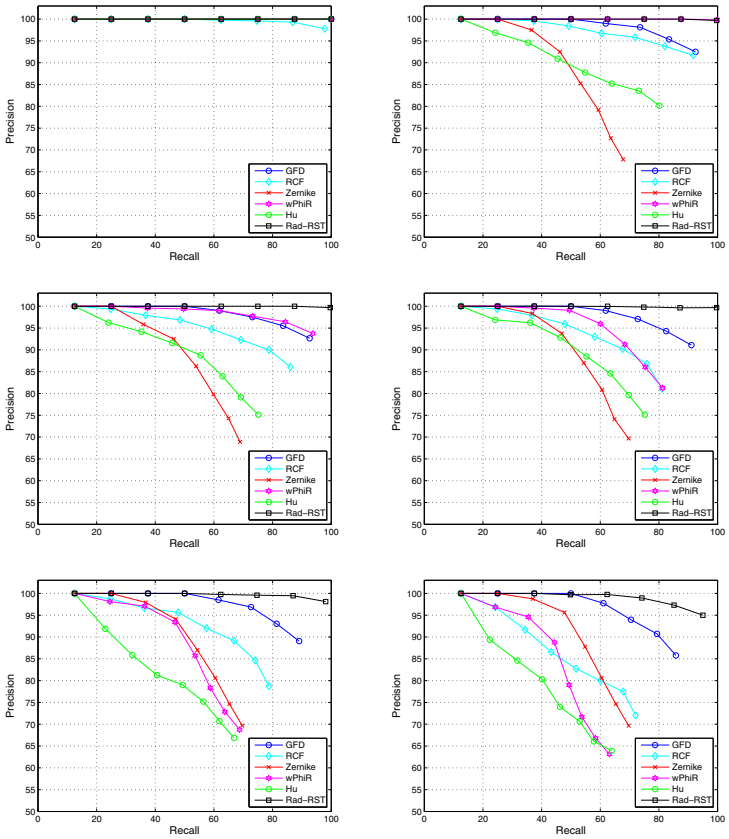

Fig. 10. $Pr - Re$ curves of comparison descriptors on the six logo datasets. Noise densities vary from d = 0 to d = 0.20 with an increment of 0.04 for the six figures from left to right and from top to bottom.

Table 2. Average running time for each descriptor and similarity measure computation for a single pair of shape images in Shapes99 database

	GFD	RCF	Zernike	W$\Phi\Re$	Hu	$\Re$-RST
Runtime (sec.)	0.87	0.32	1.97	0.85	0.15	3.15

is. As far as concern to computational cost, the observed average running time (including descriptor and similarity measure computation times) for all methods and for one pair of images is provided in Table 2.

6 Conclusion

In this paper, we have developed a method of finding RST parameters from Radon projections. This is of particular interest in domains where only image

projections are provided, as in medical or industrial computed tomography. We have described in details and motivated the extended version of Radon transform on $[0, 2\pi]$ to deal with rotation in $[-\pi, \pi]$. We have also used this method for a pattern recognition task where the recognition rates testify its superiority to well known and powerful descriptors. Extension of the method to other geometric transformations are interesting topics for further investigations.

References

1. Zhang, D., Lu, G.: Review of shape representation and description techniques. Pattern Recognition 37(1), 1–19 (2004)
2. Tabbone, S., Wendling, L., Salmon, J.-P.: A new shape descriptor defined on the Radon transform. Computer Vision and Image Understanding 102, 42–51 (2006)
3. Wang, X., Xiao, B., Ma, J.-F., Bi, X.-L.: Scaling and rotation invariant analysis approach to object recognition based on Radon and Fourier-Mellin transforms. Pattern Recognition 40(12), 3503–3508 (2007)
4. Chen, Y.W., Chen, Y.Q.: Invariant Description and Retrieval of Planar Shapes using Radon Composite Features. IEEE Trans. on Signal Processing 56(10), 4762–4771 (2008)
5. Nacereddine, N., Tabbone, S., Ziou, D., Hamami, L.: Shape-based image retrieval using a new descriptor based on the Radon and wavelet transforms. In: 20th Intern. Conf. on Pattern Recognition, pp. 1997–2000 (2010)
6. Hjouj, F., Kammler, D.W.: Identification of Reflected, Scaled, Translated, and Rotated Objects from their Radon Projections. IEEE Trans. on Image Processing 17(3), 301–310 (2008)
7. Wan, Y., Wei, N.: A Fast Algorithm for Recognizing Translated, Rotated, Reflected, and Scaled Objects from only their Projections. IEEE Signal Processing Letters 17(1), 71–74 (2010)
8. Deans, S.R.: The Radon Transform and Some of its Applications. John Wiley & Sons, New York (1983)
9. Shepp, L.A., Logan, B.F.: Fourier reconstruction of a head section. IEEE Trans. Nuclear Sci. 21(3), 21–44 (1974)
10. Sebastian, T.B., Klein, P.N., Kimia, B.B.: Recognition of Shapes by Editing Shock Graphs. In: 8th Intern. Conference on Computer Vision, pp. 755–762 (2001)
11. Doermann, D.S., Rivlin, E., Weiss, I.: Applying algebraic and differential invariants for logo recognition. Machine Vision and Applications 9(2), 73–86 (1996)
12. Teh, C.H., Chin, R.T.: On image analysis by the method of moments. IEEE Trans. on Pattern Analysis and Machine Intelligence 10(4), 496–513 (1988)
13. Khotanzad, A., Hong, Y.H.: Invariant image recognition by Zernike moments. IEEE Trans. on Patt. Anal. and Mach. Intell. 12(5), 489–497 (1990)
14. Zhang, D., Lu, G.: Shape-based image retrieval using generic Fourier descriptor. Signal Processing: Image Communication 17(10), 825–848 (2002)
15. Jafari-Khouzani, K., Soltanian-Zadeh, H.: Rotation-invariant multiresolution texture analysis using Radon an wavelet transforms. IEEE Trans. on Image Processing 14(6), 783–795 (2005)